AIAA 82-4185

Ocean Cable Dynamics Using an Orthogonal Collocation Solution

Herman Migliore* and Ernest McReynolds†
Portland State University, Portland, Ore.

Ocean cable systems are particularly vulnerable to failure during deployment and retrieval operations due to dynamic effects imposed by ship motion and time dependent changes in hydrodynamic forces, cable length, area, and tension. The continuous equations of motion for a cable system undergoing change of length were developed, where hydrodynamic forces were incorporated as added mass and velocity-squared drag. The nonlinear equations were solved using method of weighted residuals, orthogonal collocation. Residual quantities were not treated directly; rather, an approximation procedure for spatial derivatives was developed resulting in broader application for the solution technique. Numerical results were compared with two sets of available experimental data. Both experiments involved laboratory-scale cable systems in a one-dimensional variable length configuration and in two-dimensional fixed length configurations. Analytic and experimental results were in reasonable agreement with some differences attributed to defining coefficient of drag as a constant, modeling difficulties, and low-order numerical approximation.

Introduction

OCEAN cable systems are ubiquitous. Cables are used to lower and lift objects, for mooring and towing, and as members in undersea arrays. The deployment phase of cable operations can be the most critical, as exemplified by many cases of cable failure occurring during deployment and retrieval operations. The capability to analyze and design cable systems during the deployment and retrieval phase must encompass the dynamic effects of paying out and reeling in the cable system. Cable payout and reel-in includes the analysis of cable behavior under the influence of time dependent changes in length, tensions, and hydrodynamic forces.

Past cable payout/reel-in has been treated preponderantly in a quasidynamic manner.[1] With this quasidynamic approach, a dynamic analysis was performed at a fixed length for several lengths of cable. These sets of results were intended to characterize cable behavior under conditions of changing lengths. More recently, spatially discrete methods, such as lumped parameter and finite element, have been employed in a manner where length of cable system is changed at each time integration step.[2] Because of convergence considerations, adjustments present a rather abrupt change in configuration and, as a result, numerical oscillations can be introduced.

Alternately, cable systems undergoing changing length can be treated in a continuous fashion where full dynamic effects due to payout or reel-in are considered.[3] Discrete changes in system configuration can be avoided by analysis of a continuous domain. In view of this advantage, the objectives of this work were 1) develop the two dimensional continuous equations of motion for a cable system undergoing change of total length, area, and mass with time; 2) solve these equations; and 3) compare the solution with available experimental results.

Equations of Motion

A cable of finite length is situated in a three-dimensional frame of reference such that the curve of the center of the cable lies within a fixed plane which is perpendicular to the horizontal. This inertial frame is described by a right-hand Cartesian coordinate system having the customary basis $(\boldsymbol{i},\boldsymbol{j},\boldsymbol{k})$ where the x,z plane is taken parallel to the horizontal, the positive y axis is directed upward, and the plane of the cable center is the x,y plane.

Taking the inextended length of the cable as a material coordinate s, parametrization of the preceding makes the position vector of points lying on the curve

$$r=r(s,t)$$

for $0\le s\le\lambda$, where λ is the unstretched cable length and t represents time.

Differentiating r with respect to the material parameter s, assuming that $\partial r/\partial s$ does not vanish, and dividing that derivative by its magnitude, the unit tangent vector t to the curve of the cable center is obtained, i.e.,

$$t=\frac{\partial r}{\partial s}\Big/\left|\frac{\partial r}{\partial s}\right|$$

By assumption $r\cdot k=0$, therefore, $\partial r/\partial s\cdot k=0$ and, hence, $t\cdot k=0$. Thus, rotating the vector t in the x,y plane by $-\pi/2$ rad in that plane, a unit vector n perpendicular to t is produced. Since the system of coordinates is right hand, we have $k=n\times t$, and the vector set (k,n,t) serves as a local orthonormal basis for points of $r(s,t)$, $0\le s\le\lambda$. Figure 1 represents the described system at some fixed time, with vector quantities denoted with arrows in Figs. 1 and 2.

Assume that for $0\le s\le\lambda$, the plane perpendicular to t cuts the cable in such a way that the obtained cross-sectional region is approximately circular and of radius $r(s,t)$. Then, for the parameter θ, $0\le\theta\le2\pi$, where θ is the angle measured counterclockwise from k lying in the plane of that cross section, the position vector, $R(s,t)$, of a point on the surface of the cable as seen in Fig. 2 is given by

$$R(s,t)=r(s,t)+r(s,t)\,(\cos\theta k+\sin\theta n)$$

Naturally, it is assumed that the cable does not intersect itself on its surface.

With R as defined earlier the outward oriented incremental element of surface area $d\alpha$ of the cable is readily expressible as

$$d\alpha=\left[\frac{\partial R}{\partial\theta}\times\frac{\partial R}{\partial s}\right]d\theta ds \tag{1}$$

Received April 6, 1981; revision received Nov. 16, 1981. This paper is declared a work of the U.S. Government and therefore is in the public domain.

*Associate Professor of Mechanical Engineering.
†Research Associate.

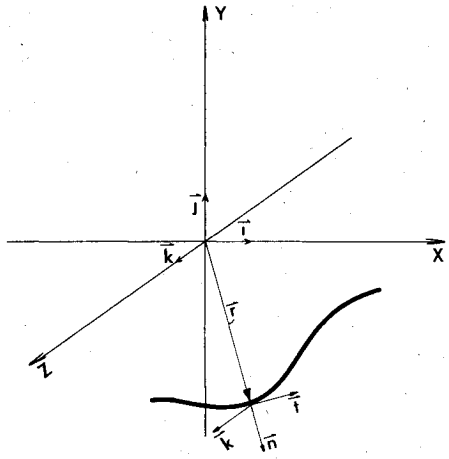

Fig. 1 Inertial frame of reference.

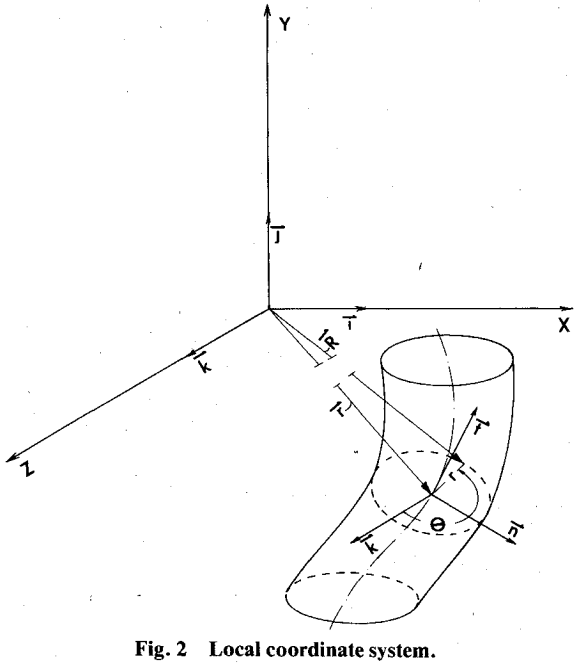

Fig. 2 Local coordinate system.

Expanding Eq. (1) yields

$$d\alpha = r\left[-\frac{\partial r}{\partial s}t + \left|\frac{\partial r}{\partial s}\right|(\cos\theta k + \sin\theta n)\right.$$

$$\left. -r\sin^2\theta\left(k\times\frac{\partial n}{\partial s}\right) + r\sin\theta\cos\theta\left(n\times\frac{\partial n}{\partial s}\right)\right]d\theta ds \tag{2}$$

Equation (2) may be further simplified by noting that

$$k\times\frac{\partial n}{\partial s} = \frac{\partial t}{\partial s};\quad n\times\frac{\partial n}{\partial s} = -\left(n\cdot\frac{\partial t}{\partial s}\right)k$$

making

$$d\alpha = r\left[-\frac{\partial r}{\partial s}t + \left|\frac{\partial r}{\partial s}\right|(\cos\theta k + \sin\theta n) - r\sin^2\theta\frac{\partial t}{\partial s}\right.$$

$$\left. -r\sin\theta\cos\theta\left(n\cdot\frac{\partial t}{\partial s}\right)k\right]d\theta ds \tag{3}$$

At this point further assumptions will be made concerning the cable. First, it is assumed that the cable is constructed of water-impermeable material; second, the cable can sustain no shearing stresses; and third, Poisson's ratio for the material composing the given cable is 1/2. The justification for these assumptions is the greatly simplified equations of motion resulting from their implementation.

From the third of the preceding requirements it can be shown[4] that for the cross-sectional area of the unstretched cable a we must have

$$a = \pi r^2\left|\frac{\partial r}{\partial s}\right|$$

Hence, the diameter d of the cable may be expressed as

$$d = 2\sqrt{\frac{a}{\pi}\left|\frac{\partial r}{\partial s}\right|^{-1}}$$

Assuming that the cable under consideration is situated wholly in water, the equation of motion for the increment of cable, $s\le\chi\le s+\Delta s$, in the inertial frame of reference is taken as

$$a\mu\Delta s\frac{\partial^2 r}{\partial t^2}(\chi,t) = T(s+\Delta s,t)t(s+\Delta s,t) - T(s,t)t(s,t)$$

$$-a\mu\Delta sgj + \left|\frac{\partial r}{\partial s}(\chi,t)\right|\Delta s[\boldsymbol{B}(\chi,t)+\boldsymbol{D}(\chi,t)] \tag{4}$$

where μ represents the mass density per unit volume of the cable, T the axial tension of the cable, and $\boldsymbol{B}$, $\boldsymbol{D}$ are the static and dynamic forces per unit length exerted on the cable by the water. The term $-a\mu\Delta sgj$ corresponds to the gravitational forces exerted on the cable element where g is the constant of uniform gravitational acceleration. Dividing Eq. (4) by Δs and taking the limit as $\Delta s\to 0$ yields

$$a\mu\frac{\partial^2 r}{\partial t^2}(s,t) = \frac{\partial}{\partial s}[T(s,t)t(s,t)] - a\mu gj$$

$$+\left|\frac{\partial r}{\partial s}(s,t)\right|[\boldsymbol{B}(s,t)+\boldsymbol{D}(s,t)] \tag{5}$$

To obtain the expression for $|\partial r/\partial s|\boldsymbol{B}$ the integral

$$-\frac{1}{\Delta s}\int_\alpha p\,d\alpha$$

is evaluated. Here α is the wet surface of the cable element and p the static pressure. With the surface datum of the water coincident with the x,z plane, for the region in which the cable lies we have

$$p = -\rho g(\boldsymbol{R}\cdot j)$$

for ρ equaling the mass density of water per unit volume. Thus,

$$\left|\frac{\partial r}{\partial s}\right|\boldsymbol{B} = \lim_{\Delta s\to 0}\frac{1}{\Delta s}\int_s^{s+\Delta s}\int_0^{2\pi}\rho g[(r\cdot j) + r\sin\theta(n\cdot j)]$$

$$\times\left[-r\frac{\partial r}{\partial s}t + r\left|\frac{\partial r}{\partial s}\right|(\cos\theta k + \sin\theta n) - r^2\sin^2\theta\frac{\partial t}{\partial s}\right.$$

$$\left. -r^2\sin\theta\cos\theta\left(n\cdot\frac{\partial t}{\partial s}\right)k\right]d\theta ds = \rho g\left[-\frac{\partial}{\partial s}(\pi r^2)(r\cdot j)t\right.$$

$$\left. -\pi r^2(r\cdot j)\frac{\partial t}{\partial s} + \pi r^2\left|\frac{\partial r}{\partial s}\right|(n\cdot j)n\right] \tag{6}$$

which, substituting $a=\pi r^2\,|\partial r/\partial s|$ gives

$$\left|\frac{\partial r}{\partial s}\right|B=a\rho g\left[-\frac{\partial}{\partial s}\left(\left|\frac{\partial r}{\partial s}\right|^{-1}t\right)(r\cdot j)+(n\cdot j)n\right] \tag{7}$$

For a cable satisfying the previously stated assumptions Breslin and Goodman[5] obtained the expression for the longitudinal cable strain

$$\epsilon=\frac{1}{E}\left[\frac{T(1+\epsilon)}{a}-\rho g(r\cdot j)\right] \tag{8}$$

where ϵ represents longitudinal strain and E is Young's modulus for the material of which the cable is constructed. The preceding relation encompasses the straining effect due to hydrostatic pressure. Since $\epsilon=|\partial r/\partial s|-1$, from Eq. (8) we obtain

$$T=\left|\frac{\partial r}{\partial s}\right|^{-1}\left[Ea\left[\left|\frac{\partial r}{\partial s}\right|-1\right]+a\rho g(r\cdot j)\right] \tag{9}$$

and from Eq. (9)

$$\frac{\partial(Tt)}{\partial s}=\frac{\partial}{\partial s}\left(Ea\left|\frac{\partial r}{\partial s}\right|^{-1}\left[\left|\frac{\partial r}{\partial s}\right|-1\right]t\right)$$
$$+a\rho g\frac{\partial}{\partial s}\left(\left|\frac{\partial r}{\partial s}\right|^{-1}(r\cdot j)t\right) \tag{10}$$

Evaluating the derivative of the rightmost term of Eq. (10),

$$\frac{\partial(Tt)}{\partial s}=\frac{\partial}{\partial s}\left(Ea\left|\frac{\partial r}{\partial s}\right|^{-1}\left[\left|\frac{\partial r}{\partial s}\right|-1\right]t\right)$$
$$+a\rho g\frac{\partial}{\partial s}\left(\left|\frac{\partial r}{\partial s}\right|^{-1}t\right)(r\cdot j)+a\rho g(t\cdot j)t \tag{11}$$

For the dynamic fluid load per unit length the formulation cited by Webster[6] will be employed.

$$D=C_m\rho\frac{\pi}{4}d^2A_n+\frac{1}{2}C_n\rho d\,|V_n|V_n+\frac{\pi}{2}C_t\rho d\,|V_t|V_t \tag{12}$$

where C_m is the coefficient of added mass, C_n the normal drag coefficient, C_t the tangential drag coefficient, all three dimensionless, and d is the cable diameter. The vectors A_n, V_n, and V_t are the normal fluid particle acceleration, the normal fluid particle velocity, and the tangential fluid particle velocity, respectively. These vector quantities are formed with respect to the local system of coordinates. For a velocity field $C(r,t)$ representing a current in the inertial frame, the cited vector quantities are

$$A_n=\left[\left(\frac{dC}{dt}-\frac{\partial^2 t}{\partial t^2}\right)\cdot n-\left(\frac{\partial t}{\partial t}\cdot n\right)\left(C-\frac{\partial r}{\partial t}\right)\cdot t\right]n$$
$$V_n=\left[\left(C-\frac{\partial r}{\partial t}\right)\cdot n\right]n$$
$$V_t=\left[\left(C-\frac{\partial r}{\partial t}\right)\cdot t\right]t \tag{13}$$

From Eqs. (12) and (13),

$$\left|\frac{\partial r}{\partial s}\right|D=C_m\rho a\left[\left(\frac{dC}{dt}-\frac{\partial^2 r}{\partial t^2}\right)\cdot n-\left(\frac{\partial t}{\partial t}\cdot n\right)\left(C-\frac{\partial r}{\partial t}\right)\cdot t\right]n$$
$$+C_n\rho\sqrt{\frac{a}{\pi}\left|\frac{\partial r}{\partial s}\right|}\left|\left(C-\frac{\partial r}{\partial t}\right)\cdot n\right|\left[\left(C-\frac{\partial r}{\partial t}\right)\cdot n\right]n$$
$$+C_t\rho\sqrt{\pi a\left|\frac{\partial r}{\partial s}\right|}\left|\left(C-\frac{\partial r}{\partial t}\right)\cdot t\right|\left[\left(C-\frac{\partial r}{\partial t}\right)\cdot t\right]t \tag{14}$$

Substituting Eqs. (7), (11), and (14) into Eq. (5) yields the equation of motion for the cable in the inertial frame between its boundaries; $(0<s<\lambda)$

$$a\mu\frac{\partial^2 r}{\partial t^2}=\frac{\partial}{\partial s}\left[Ea\left|\frac{\partial r}{\partial s}\right|^{-1}\left[\left|\frac{\partial r}{\partial s}\right|-1\right]t\right]+ag(\rho-\mu)j$$
$$+C_m\rho a\left[\left(\frac{dC}{dt}-\frac{\partial^2 r}{\partial t^2}\right)\cdot n-\left(\frac{\partial t}{\partial t}\cdot n\right)\left(C-\frac{\partial r}{\partial t}\right)\cdot t\right]n$$
$$+C_n\rho\sqrt{\frac{a}{\pi}\left|\frac{\partial r}{\partial s}\right|}\left|\left(C-\frac{\partial r}{\partial t}\right)\cdot n\right|\left[\left(C-\frac{\partial r}{\partial t}\right)\cdot n\right]n$$
$$+C_t\rho\sqrt{\pi a\left|\frac{\partial r}{\partial s}\right|}\left|\left(C-\frac{\partial r}{\partial t}\right)\cdot t\right|\left[\left(C-\frac{\partial r}{\partial t}\right)\cdot t\right]t \tag{15}$$

To Eq. (15), we add the boundary conditions

$$r=U(t)\quad\text{at}\quad s=\lambda \tag{16}$$

$$M\frac{\partial^2 r}{\partial t^2}=Ea\left|\frac{\partial r}{\partial s}\right|^{-1}\left[\left|\frac{\partial r}{\partial s}\right|-1\right]t+\left(\frac{4}{3}\pi R^3\rho-M\right)gj$$
$$+C_{Lm}\rho\frac{4}{3}\pi R^3\left(\frac{dC}{dt}-\frac{\partial^2 r}{\partial t^2}\right)+C_D\rho\frac{\pi}{2}R^2$$
$$\times\left|C-\frac{\partial r}{\partial t}\right|\left(C-\frac{\partial r}{\partial t}\right)\quad\text{at } s=0 \tag{17}$$

$U(t)$ is a known vector function of time and Eq. (17) is intended to approximate the behavior of a spherical load in which M represents the mass of the load, C_{Lm} the coefficient of added mass, C_D the coefficient of drag, and R the radius of the given sphere. Assuming that all points of the cable lie below the water surface datum makes Eqs. (15-17) the equations of motion for a totally immersed cable supporting a spherical load. If, additionally, the unstretched length of the cable is allowed to vary as a function of time, $[\lambda=\lambda(t)]$, and values for $r(s,0)$, $\partial r/\partial t(s,0)$, $\partial r/\partial s(s,0)$ are provided as initial conditions for all values of the material coordinate, then Eqs. (15-17) together with these new conditions provide a system of partial-differential equations modeling an immersed cable supporting a spherical load in two dimensions subject to payout or reel-in.

In order to facilitate the finding of an approximate solution to the proceeding system by the method of orthogonal collocation it is necessary to normalize the material coordinate for the evaluation of quadratures which will be required in subsequent sections. This is accomplished by defining

$$s=\lambda(t)\sigma,\quad 0\le\sigma\le 1$$

Also, to numerically integrate second-order derivatives with respect to time in the given system we define

$$r(\lambda\sigma,t)=P(\sigma,t)\qquad\frac{\partial r}{\partial t}(\lambda\sigma,t)=V(\sigma,t)\qquad\frac{\partial r}{\partial s}(\lambda\sigma,t)=T(\sigma,t)$$

Finally, it is assumed that for all $0\le s\le\lambda(t)$ and any time t, $\partial^2 r/\partial s\partial t$ is continuous and $\partial r/\partial t$ is defined. This makes

$$\frac{\partial}{\partial t}\left(\frac{\partial r}{\partial s}\right)=\frac{\partial}{\partial s}\left(\frac{\partial r}{\partial t}\right)$$

Utilization of the preceding definitions and assumptions permits the transformation of the given second-order system

Eqs. (15-17) into a first-order system in the normalized material coordinate

$$a\mu\left[\frac{\partial V}{\partial t}-\frac{\sigma}{\lambda}\frac{d\lambda}{dt}\frac{\partial V}{\partial \sigma}\right]=\frac{Ea|T|^{-2}}{\lambda}\left[[|T|-1]\frac{\partial T}{\partial \sigma}+[2-|T|]\left(\frac{\partial T}{\partial \sigma}\cdot t\right)t\right]+ag(\rho-\mu)j$$
$$+C_m\rho a\left[\left(\frac{dC}{dt}-\frac{\partial V}{\partial t}+\frac{\sigma}{\lambda}\frac{d\lambda}{dt}\frac{\partial V}{\partial \sigma}\right)\cdot n-\frac{|T|^{-1}}{\lambda}\left(\frac{\partial V}{\partial \sigma}\cdot n\right)(C-V)\cdot t\right]n$$
$$+C_n\rho\sqrt{\frac{a}{\pi}|T|}\,|(C-V)\cdot n|\,[(C-V)\cdot n]n$$
$$+C_t\rho\sqrt{\pi a|T|}\,|(C-V)\cdot t|\,[(C-V)\cdot t]t$$
$$\text{for}\quad 0<\sigma<1 \tag{18}$$

$$P=U(t)\quad\text{at}\quad\sigma=1 \tag{19}$$

$$M\frac{\partial V}{\partial t}=Ea|T|^{-1}[|T|-1]t+\left(\frac{4}{3}\pi R^3\rho-M\right)gj$$
$$+C_{Lm}\rho\frac{4}{3}R^3\left(\frac{dC}{dt}-\frac{\partial V}{\partial t}\right)+C_D\rho\frac{\pi}{2}R^2|C-V|(C-V)$$
$$\text{at}\quad\sigma=0 \tag{20}$$

$$\frac{\partial P}{\partial t}=V+\frac{d\lambda}{dt}T\quad\text{for}\quad 0\le\sigma\le 1 \tag{21}$$

$$\frac{\partial T}{\partial t}=\frac{1}{\lambda}\frac{\partial V}{\partial \sigma}+\frac{\sigma}{\lambda}\frac{d\lambda}{dt}\frac{\partial T}{\partial \sigma}\quad\text{for}\quad 0\le\sigma\le 1 \tag{22}$$

and $P(\sigma,0)$, $V(\sigma,0)$, $T(\sigma,0)$ are specified initially. Note that in the preceding C and dC/dt are evaluated where P is substituted for r and the corresponding time derivative is formed, and that t and n are invariant for the given transformation.

Numerical Solution

To approximate the solutions of the normalized system of equations a weighted residual method (MWR) is employed. In particular, the technique of orthogonal collocation is implemented due to the ease with which the problem may be formulated for solution on a digital computer.

Essentially, orthogonal collocation is a discrete approximation to the solution by the method of Galerkin.[7] For example, trial solutions satisfying initial conditions of the normalized system are assumed

$$P(\sigma,t)=\sum_{k=0}^{m}a_k(t)P_k(\sigma)$$
$$V(\sigma,t)=\sum_{k=0}^{n}b_k(t)P_k(\sigma)$$
$$T(\sigma,t)=\sum_{k=0}^{q}c_k(t)P_k(\sigma)$$

in which the functions $P_k(\sigma)$ are elements of a complete set of basis functions on the interval (0,1). The expansions for P, V, and T are substituted into Eqs. (18), (21), and (22) to form interior error residuals, $E_1(\sigma,t)$, $E_2(\sigma,t)$, and $E_3(\sigma,t)$, respectively. Of these we require that

$$\int_0^1\sigma(1-\sigma)E_i(\sigma,t)P_k(\sigma)d\sigma=0 \tag{23}$$

for $i=1, 2, 3$ and $k=0,\ldots,$ max $(m, n, q)-2$. Additionally, boundary conditions, Eqs. (19) and (20), must be satisfied upon substitution of the trial solutions as well as Eqs. (21) and (22) for $\sigma=0$ and $\sigma=1$. By implementing this scheme the normalized material coordinate is eliminated from the system of partial-differential equations and a new system of time varying ordinary-differential equations is obtained, the solutions of which would provide the coefficient vectors $a_k(t)$, $b_k(t)$, and $c_k(t)$ and, hence, an approximate solution to the normalized system.

Although the Galerkin method may promise an excellent approximate solution to the given set of partial-differential equations,[7] the success of its use depends heavily upon the feasibility in carrying out the integrations of Eq. (23) to obtain a system in the coefficient vectors. Clearly, for the given system this is a formidable task. However, by the performance of numerical quadratures to evaluate these definite integrals this difficulty can be circumvented with the acceptance of error due to the approximate nature of such integration.

At this point the trial solutions will be taken as polynomial expansions in σ, where $P_k(\sigma)$ denotes that polynomial of the complete set of degree k. This is done to simplify the evaluation of $P_k(\sigma)$ on the computer. Note also that this requires $m=n$ and $q=n-1$ for the trial solutions since these also must satisfy Eqs. (21) and (22).

From the integral inner product associated with the nonhomogeneous Galerkin solution follows naturally the integrating weight, $W(\sigma)=\sigma(1-\sigma)$, for which is constructed an $n-1$ order Gaussian quadrature on (0,1). This reduces the integrals of Eq. (23) to

$$\int_0^1\sigma(1-\sigma)E_i(\sigma,t)P_k(\sigma)d\sigma=\sum_{j=1}^{n-1}W_jE_i(\sigma_j,t)P_k(\sigma_j)=0$$
$$i=1,2,3\qquad k=0,\ldots,n-2 \tag{24}$$

Here the σ_j will be distinct points lying in (0,1) and the W_j will be positive weights.[8]

Since the $P_k(\sigma)$ are selected from a complete set of polynomials, the $(n-1)\times(n-1)$ matrix $[Q_{kj}]$, for $Q_{kj}=P_k(\sigma_j)$, will be composed of $n-1$ linearly independent functions evaluated at $n-1$ distinct points and, hence, invertible. Thus, for the linear homogeneous systems of equations appearing in Eq. (24), we must have the solution

$$E_i(\sigma_j,t)=0\ \text{for}\ i=1,2,3;\quad j=1,\ldots,n-1 \tag{25}$$

Adding the points $\sigma_0=0$, $\sigma_n=1$, to the given σ_j values one obtains the set of so-called orthogonal collocation points. Equation (25) together with the boundary conditions, Eqs. (19) and (20), and Eqs. (21) and (22) evaluated at the points σ_0 and σ_n, provide a time varying system of $3n+3$ ordinary-differential equations in the $5n+5$ variables

$$P(\sigma_j,t),\quad V(\sigma_j,t),\quad \frac{\partial V}{\partial \sigma}(\sigma_j,t)$$
$$T(\sigma_j,t),\quad \frac{\partial T}{\partial \sigma}(\sigma_j,t)\quad\text{for}\ j=0,\ldots,n$$

The solutions of this system would provide us with approximate solutions of the normalized partial-differential system at the collocation points. To do this, the values for $\partial V/\partial\sigma(\sigma_j,t)$, $\partial T/\partial\sigma(\sigma_j,t)$ must be expressed in terms of the remaining variables.

Historically, derivatives with respect to the normalized material coordinate may be eliminated through the application of a technique due to Finlayson.[9] For example, rearranging the terms of the trial solution for $V(\sigma,t)$ and differentiating with respect to σ yields

$$V(\sigma,t) = \sum_{k=0}^{n} \beta_k(t)\sigma^k \tag{26}$$

$$\frac{\partial V}{\partial \sigma}(\sigma,t) = \sum_{k=0}^{n} \beta_k(t) k\sigma^{k-1} \tag{27}$$

Evaluating these quantities at the collocation points provides the relations

$$V(\sigma_j,t) = \sum_{k=0}^{n} \beta_k(t)\sigma_j^k \tag{28}$$

$$\frac{\partial V}{\partial \sigma}(\sigma_j,t) = \sum_{k=0}^{n} \beta_k(t) k\sigma_j^{k-1} \quad \text{for} \quad j=0,\ldots,n \tag{29}$$

Equation (28) is a linear system of equations having the coefficient matrix $[H_{jk}]$, $H_{jk}=\sigma_j^k$, which is composed of $n+1$ linearly independent functions evaluated at $n+1$ distinct points. Hence, the vectors $\beta_k(t)$ may be expressed in terms of the value of the function $V(\sigma,t)$ at the collocation points. Substituting these values into the expressions for $\partial V/\partial\sigma(\sigma_j,t)$ provides expansions for these values in terms of the values $V(\sigma_j,t)$.

When the same procedure is attempted to evaluate the values $\partial T/\partial\sigma(\sigma_j,t)$ it fails since, due to the degree limitations imposed on the trial solution for $T(\sigma,t)$, too many sample points lie in (0,1) for a unique determination of the corresponding coefficient vectors. This may be remedied by noting that the Gaussian quadrature of Eq. (24) with the integrating weight $\sigma(1-\sigma)$ generates the same sample points as those interior sample points for the Lobatto quadrature with unit integrating weight on (0,1) (Ref. 10). This quadrature is of the form

$$\int_0^1 f(\sigma)\,d\sigma = \omega_0 f(0) + \sum_{j=1}^{n-1} \omega_j f(\sigma_j) + \omega_n f(1) \tag{30}$$

for any integrable function $f(\sigma)$ on (0,1). Selecting the basis functions for the trial solutions as orthogonal polynomials on the interval just given with respect to unit weight reduces the computation of material derivatives to the evaluation of quadratures. For example, consider again the trial solution for $V(\sigma,t)$ and its derivative with respect to σ

$$V(\sigma,t) = \sum_{k=0}^{n} b_k(t)P_k(\sigma), \quad \frac{\partial V}{\partial \sigma}(\sigma,t) = \sum_{k=0}^{n} b_k(t)\frac{dP_k(\sigma)}{d\sigma}$$

To obtain the coefficient vectors appearing in the left expression we exploit the orthogonality property of the expansion polynomials. To obtain $b_k(t)$ we have

$$\int_0^1 V(\sigma,t)P_k(\sigma)\,d\sigma = \sum_{i=0}^{n} b_i(t)\int_0^1 P_i(\sigma)P_k(\sigma)\,d\sigma \tag{31}$$

If, additionally, the polynomials are normalized over the interval of integration the computations are greatly simplified and Eq. (31) becomes

$$\sum_{j=1}^{n} \omega_j V(\sigma_j,t)P_k(\sigma_j) = b_k(t) \tag{32}$$

upon employing the Lobatto quadrature of Eq. (31). From the preceding $\partial V/\partial\sigma(\sigma,t)$ may now be expressed in terms of the value of $V(\sigma,t)$ at the collocation points.

Clearly this technique is equally applicable to the lower order expansion of the trial solution for $T(\sigma,t)$, however, for low values of n another difficulty may evidence itself. This may be seen by noting that the quadrature of Eq. (32) is exact only for polynomials of degree less than or equal to $2n-1$ (Ref. 8). Necessarily, this introduces error in the evaluation of $\partial V/\partial\sigma(\sigma,t)$, since the integrand of the left-hand member of Eq. (31) for $k=n$ is of order $2n$. In practice this error rapidly diminishes with increasing n and no significant problems evidenced themselves for approximate solutions of order greater than or equal to 10. A benefit of this technique is that the orthogonal polynomials determined by the integrating weight $W(\sigma)\equiv 1$ are the shifted Legendre polynomials. For these and the associated normalized polynomials there are convenient recursion relations by which the values $P_k(\sigma_j)$, $dP_k/d\sigma(\sigma_j)$ may be evaluated easily on the computer.

Employing the techniques just described a computer program was written integrating in time the resultant system of differential equations. Anticipating a relatively "stiff" system of equations for a number of the cable models to be simulated, indicated that a strongly stable integration technique was needed. For this reason an Adams-Bashforth fourth-order predictor-corrector algorithm with fourth-order Runge-Kutta start-up was selected.

Comparison to Available Experimental Data

In order to gain confidence in applying the developed computer program, a set of experimental data was sought for comparison purposes. Data was found to be available from two sets of laboratory-scale experiments.[11,12] Even though these experimental systems were not full scale relative to most ocean cable systems, the controlled test conditions were desirable from a comparison standpoint. Both sets of tests involved one piece of cable with a 50.8-mm (2-in.) diameter load at one end. The disposition of the other end of the cable depended on the particular test configuration. Two types of cable materials were employed for the purpose of simulating a relatively stiff and relatively soft cable. One cable was solid rubber with a diameter of 4.04 mm (0.159 in.), a weight of 13.7 g/m (0.0092 lb/ft) in air, and an *Ea* (elastic modulus times cross-sectional area), that was estimated to be a constant of 9 N (2.0 lbf). The other cable was braided nylon with a diameter of 1.50 mm (0.059 in.), a weight of 1.18 g/m (0.000792 lb/ft) in air, and an *Ea* that was estimated to be a constant of 1000 N (225 lbf). Both cables were used in the two test configurations, one-dimensional variable length[11] and two-dimensional fixed length.[12]

One-Dimensional Variable Length

The variable length test involved hanging the cable straight down in a tank with the spherical load at the bottom end of the cable. The load in this case weighed 445.4 g (1.003 lb) in water. The surface end of the cable was attached to a winching mechanism, mounted on a platform which was moveable in a vertical direction. In this manner the cable system could be paid-out, reeled-in, or subjected to simulated ship motion. The winching mechanism provided a measure of cable payout/reel-in velocity at the surface and a load cell mounted near the surface gave a measure of tension.

The computer program was exercised with several test variations: each cable type, both reel-in and payout, "crash stop" conditions, and with and without simulated ship motion. Typical comparisons of results can be seen in Figs. 3 and 4. Tensions at the top of the cable (water surface) are plotted relative to time. Figure 3 shows rubber cable initially at 1.52 m (5 ft) under payout conditions with no ship motion. Figure 4 shows nylon cable initially at 16.7 m (55 ft) under reel-in conditions with no ship motion. The initiation of payout and reel-in involved analogous accelerations. Specifically, the cables were started from a velocity of zero and achieved a steady velocity of 0.61 m/s (2 ft/s), within 0.7 s. As can be seen in both tests, dynamic tension effects were

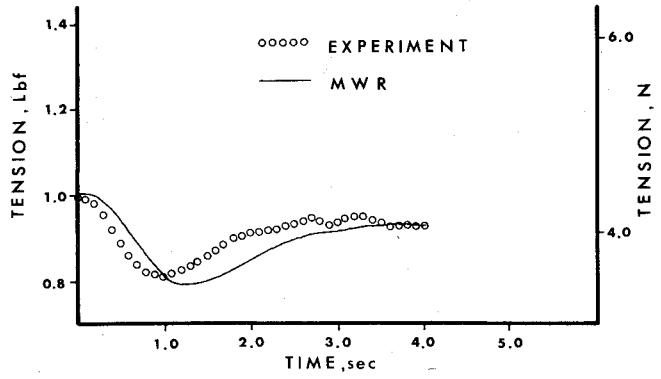

Fig. 3 Tension history at top, rubber cable payout.

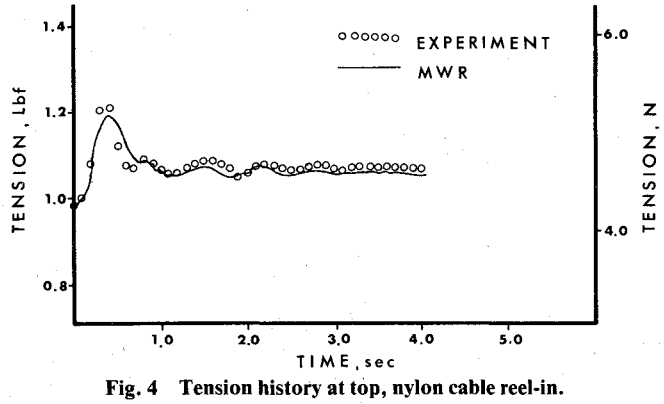

Fig. 4 Tension history at top, nylon cable reel-in.

induced by initiation of payout and reel-in, with steady-state tension resulting after about 3 s. Within the first 2 s, tension dropped by about 20% during payout initiation and tenson raised by about 20% during reel-in initiation.

Figure 3 shows general agreement between experimental and analytical results (MWR). A phase shift of about 0.2 s is evident resulting in an amplitude difference of about 15% of the steady tension value. These differences could be attributed to using a constant value for the cable elastic modulus or using constant values for coefficient of drag. A commonly used value of 0.5 (Ref. 13) was used for coefficient drag of the spherical load. The coefficient of tangential drag on the rubber cable was assumed to be negligible. From an intuitive stand, this assumption was reasonable considering the relative length of the cable in the overall system and considering the smooth skin of the cable. Furthermore, examination of the experimental results revealed that change in steady-state tension could be accounted for effectively by the change in cable weight due to payout or reel-in.

Alternatively, the coefficient of tangential drag for nylon cable was found to be 0.01 as determined from the net drag force which was calculated from the steady-state tension minus the change in cable weight in water. Figure 4 shows comparison of experimental and analytic (MWR) results for nylon cable reel-in. Slight period and phase differences are revealed; amplitude differences are about 10% relative to steady tension values. Again, constant values for coefficient of drag and cable modulus were used, as defined previously.

Two other factors should be considered in comparing these results to experimental data and tantamountly for general-purpose application of the developed method. The MWR results shown in Figs. 3 and 4 were based on using 10 collocation points. In general, more collocation points tend to increase accuracy and "soften" results; however, more collocation points require smaller increments during time integration. The other significant factor is simulation of acceleration profile during initiation of payout or reel-in. For

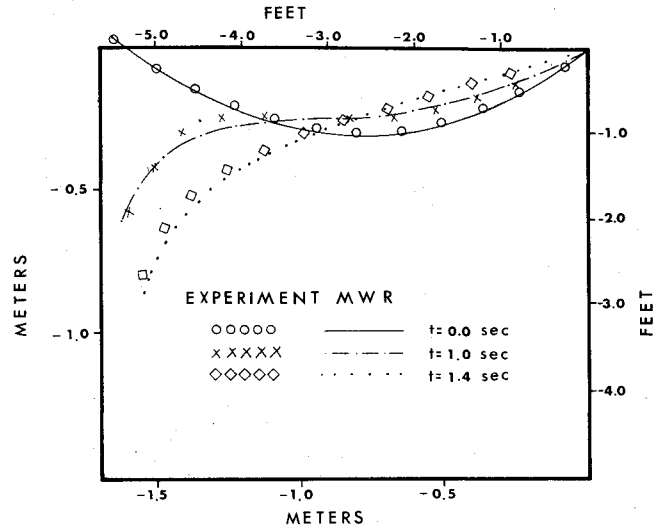

Fig. 5 Displacement history, rubber cable, anchor last deployment.

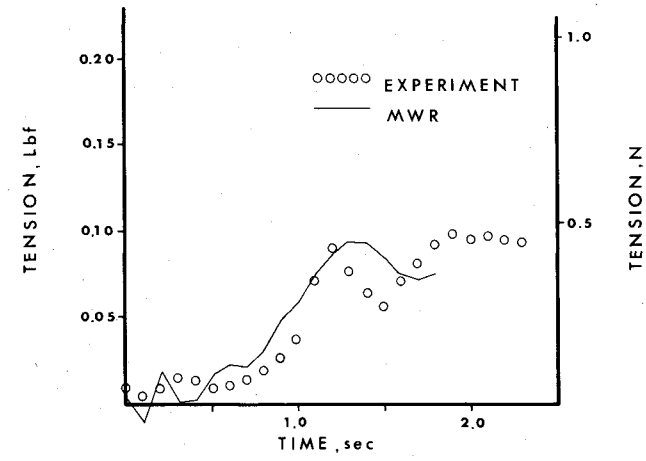

Fig. 6 Tension history at fixed end, rubber cable, anchor last deployment.

most ocean applications, exact acceleration data is not available a priori. When such data is available, an appropriate numerical representation, such as a cubic spline, could be utilized to precisely define the payout/reel-in velocity boundary condition. Because of the potential difficulty in obtaining acceleration data, a generalized step function procedure was developed. The MWR results shown is Figs. 3 and 4 employed this generalized step function approach for defining payout/reel-in acceleration.

Two-Dimensional Fixed Length

The other set of experiments involved fixed cable lengths as part of laboratory sized systems. Even though the variable length aspect was lacking, these experiments did provide a rather complex exercise in defining initial configuration and modeling two-dimensional dynamic behavior. The cable systems were composed of either a nylon or rubber cable of about 1.8 m (6 ft) in length with a spherical load at one end of the cable. Comparisons were made on two test conditions: buoy relaxation and simulated anchor-last deployment.

In the buoy relaxation, one end of the cable is attached to the bottom and the spherical load is attached to the other end. In this case, the load was positively buoyant -0.54 N (-0.12 lbf). The load, and top of the cable, were displaced a prescribed amount and allowed to return to equilibrium, all of which occurs in water. In the anchor last experiment, the cable is positioned along the surface in a catenary like

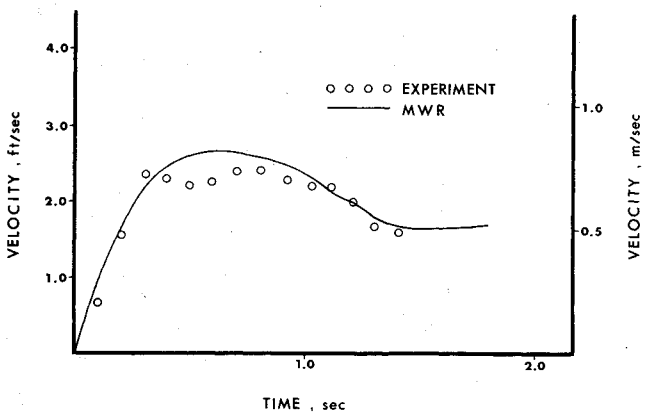

Fig. 7 Velocity history at load end, rubber cable, anchor last deployment.

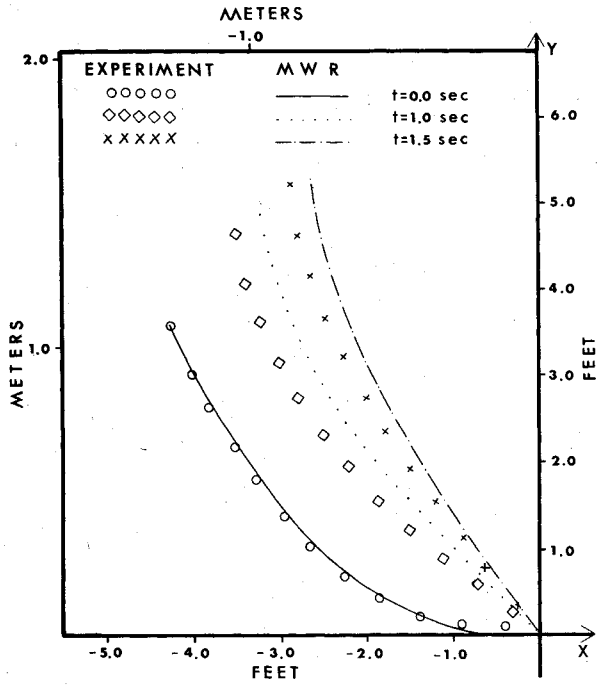

Fig. 8 Displacement history, nylon cable, buoy relaxation.

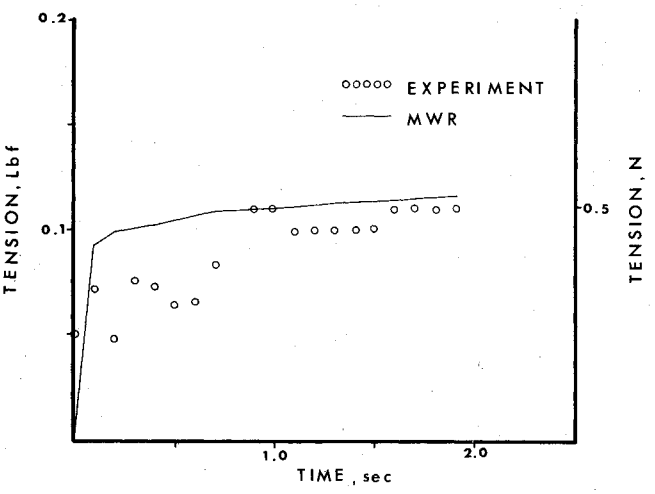

Fig. 9 Tension history at fixed end, nylon cable, buoy relaxation.

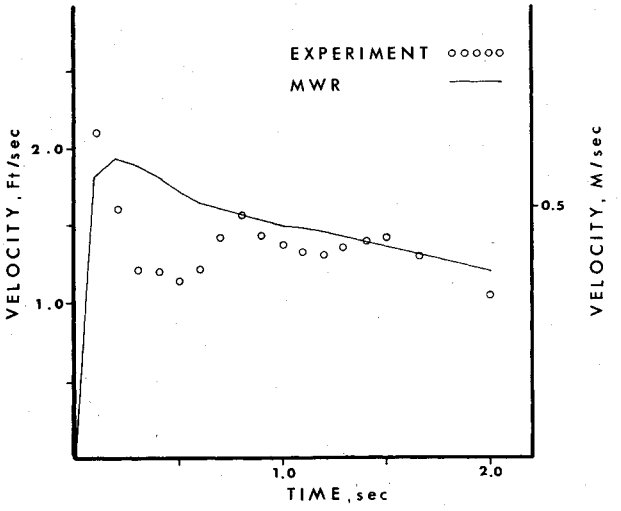

Fig. 10 Velocity history at buoy, nylon cable, buoy relaxation.

fashion. One end of the cable is fixed at the surface and the other end is attached to the load which is temporarily held at the surface. The load, in this case, is negatively buoyant (0.48 N, 0.108 lb) and is released from the surface and allowed to free fall in water with the cable attached.

As seen in Figs. 5-10, MWR was compared to experimental results for both test conditions. Results include displacement history of cable, tension at the fixed end of the cable and velocity at the load end of the cable. Coefficients of drag were the same as in the variable length cases. In addition, the coefficient of normal drag was considered to be 1.35 (Ref. 13). Coefficients of added mass were 1.00 for the cable and 0.5 for the load.[13]

Figures 5-7 show the experimental and MWR results for rubber cable undergoing simulated anchor-last deployment. Figure 5 shows displacement history. The initial configuration is seen at time equal to zero. The load was released, and displacements at 1.0 and 1.4 s are shown. The general shape of the MWR reasonably compares to the experimental positions. MWR, however, appears to be leading the experimental data, which can be attributed to using constant values for coefficients of drag (and added mass). Figure 6 shows tension history at the fixed end. Again, the salient MWR responses compare with experimental. The overshoot near the beginning is numerical in nature. In general, a greater number of collocation points tend to control overshoot, with an upper limit dependent on integration time step and word size of the computer. Twenty- five collocation points were used in the rubber anchor last analysis. Another factor is negative tension at the time of load release. In the case of MWR response, cable bending stiffness is lacking and out-of-plane motion is not accounted for. These factors coupled with a near neutrally buoyant cable induce negative analytic tension. The experimental data did not display such behavior. Also the triaxial tension transducer and cable are joined with an in-line connection. This additional boundary constraint overdetermines the analytic system model. Figure 7 compares velocity at load for MWR and experimental data. The experiment appears to be undergoing velocity oscillations which do not appear in MWR. Analysis by other numerical techniques, finite element and lumped parameter,[13] exhibit a similar disagreement. Rotation and whipping of the load is not modeled explicitly and may contribute to this disagreement, especially since velocity is measured at the load.

Figures 8-10 compare experimental and MWR results for nylon undergoing buoy relaxation conditions. The displacement history, Fig. 8, again shows MWR generally leading the experiments. Nonetheless, the form of both displacement curves favorably compare. Figure 9 shows tension at the fixed end. Unlike the anchor last comparisons, MWR displays relatively smooth behavior. Twenty-five

collocation points are sufficient for modeling buoy relaxation behavior, with no overshoot problems. The tension oscillations in the experimental results may be attributed in part to the complex cable-transducer connection which cannot be modeled by a second-order partial-differential equation. Figure 10 shows velocity at the load for the buoy relaxation. Again, oscillation in experimental velocity deviated from the smooth MWR result indicating the possibility of load dependent effects, or, differentiation errors associated with experimental processing.

MWR was also compared to available finite element results[13] for the anchor last and buoy relaxation configurations. Finite element exhibited stiffer response relative to MWR and experimental values, as would result if the order to finite element approximation was too low. A valid comparison of the two numerical techniques would require similar orders of approximation and they would be expected to converge.[14]

Conclusions and Recommendations

As exemplified by experimental results, the transient effects of initiating payout or reel-in of ocean cable systems can be significant. Two-dimensional equations of motion for a cable with end loads were developed where these equations accounted for deterministic ship motion and change of cable length with time. Hydrodynamic forces were modeled as acceleration dependent added mass and velocity-squared drag. Load dependent change of cable area was also incorporated.

Spatial solution was performed over the entire cable domain using the method of weighted residual, orthogonal collocation. Residuals were not treated directly, but rather approximations for spatial derivatives were developed, thus permitting versatility in application to other partial-differential equations. Time integration was performed effectively by using a conventional Adams technique.

Comparison of analytic to one-dimensional variable length and two-dimensional fixed length experimental results show general agreement. Point-to-point disagreement did exist, but was basically attributed to difficulties in defining drag, added mass, or in lacking explicit modeling of experimental boundary conditions.

Future work should include an integrated fluid-cable approach to avoid problems with defining drag and added mass. Load dependent properties are important for composite cable materials. Additional degrees of freedom may be necessary for complex boundary loads and constraints. Additional comparison to other analytic results and experimental data are important to further develop the computer program into a design tool.

Acknowledgments

This work was substantially funded by Office of Naval Research, Ocean Technology Branch under Contract N0014-78-C-0631. The cooperation of the Division of Engineering and Mechanical Engineering at Portland State are also appreciated.

References

[1] Migliore, H. J. and Zwibel, H. J., "Rigorous Treatment of Cable Systems which Change Length with Time," Civil Engineering Lab., Naval Construction Battalion, Pt. Hueneme, Calif., TM M-44-76-8, Jan. 1976.

[2] Webster, R. L., "Nonlinear Static and Dynamic Response of Underwater Cable Structures Using the Finite Element Method," Offshore Technology Conference, Houston, Tex., Paper OTC 2322, May 1975.

[3] Migliore, H. J. and Zwibel, H. J., "Dynamic Treatment of Cables which Change Length with Time," Sixth Canadian Congress on Applied Mechanics, Vancouver, B.C., Can., May 1977.

[4] Timoshenko, S. P. and Goodier, J. N., *Theory of Elasticity*, 3rd Ed., McGraw-Hill, New York, 1970, p. 486.

[5] Goodman, T. R. and Breslin, J. P., "Statics and Dynamics of Anchoring Cables in Waves," *Journal of Hydronautics*, Vol. 10, Oct. 1976, pp. 113-120.

[6] Webster, R. L., "An Application of the Finite Element Method to the Determination of Nonlinear Static and Dynamic Responses of Underwater Cable Structures," General Electric Heavy Military Equipment Dept., Syracuse, N.Y., R76EMH2, Jan. 1976.

[7] Villadsen, J. and Michelsen, M. L., *Solution of Differential Equation Models by Polynomial Approximation*, Prentice-Hall, Englewood Cliffs, N.J., 1978.

[8] Hamming, R. W., *Numerical Methods for Scientists and Engineers*, 2nd Ed., McGraw-Hill, New York, 1973, Chap. 19.

[9] Finlayson, B. A., *The Method of Weighted Residuals and Vibrational Principles*, Academic Press, New York, 1972, Chap. 5.

[10] Stroud, A. H. and Secrest, D., *Gaussian Quadrature Formulas*, Prentice-Hall, Englewood Cliffs, N.J., 1966.

[11] Ward, T. M., "Experimental Study of the Dynamics of Variable Cable Systems," Graduate Aeronautical Lab., California Institute of Technology, Pasadena, Calif., HSWT01129, 1979.

[12] Meggitt, D. J., Palo, P. A., Buck, E. F., and Lacroce, P., "Small Size Laboratory Experiments on the Large Displacement Dynamics of Cable Systems," Civil Engineering Lab., Naval Construction Battalion, Pt. Hueneme, Calif., TM M-44-78-11, June 1978.

[13] Palo, P. A., "Comparisons Between Small Scale Cable Dynamic Experimental and Simulations Using SEADYN and SNAPLG Computer Model," Civil Engineering Lab., Naval Construction Battalion, Pt. Hueneme, Calif., TM M-44-79-5, Jan. 1979.

[14] Migliore, H. J. and Webster, R. L., "Current Methods for Analyzing Dynamic Cable Responses," *The Shock and Vibration Digest*, Vol. 11, June 1979, pp. 3-16.